Anisotropic Interpolation on Graphs: The Combinatorial Dirichlet Problem

Leo Grady[1] and Eric L. Schwartz[2]

July 21, 2003

[1] L. Grady is with the Department of Cognitive and Neural Systems, Boston University, Boston, MA 02215, E-mail: lgrady@cns.bu.edu

[2] E. L. Schwartz is with the Departments of Cognitive and Neural Systems and Electrical and Computer Engineering, Boston University, Boston, MA 02215, E-mail: eric@bu.edu

Abstract

The combinatorial Dirichlet problem is formulated, and an algorithm for solving it is presented. This provides an effective method for interpolating missing data on weighted graphs of arbitrary connectivity. Image processing examples are shown, and the relation to anisotropic diffusion is discussed.

1 Introduction

Uniformly sampled images are conventionally represented via 4-connected or 8-connected (Cartesian) grids. However space-variant images require a more flexible image topology. In previous work, the use of a graph representation has been found to be useful for representing images whose resolution and local topology is not constant [1].

Space-variant sampling of visual space is ubiquitous in the higher vertebrate visual system [2]. In computer vision, this architecture is of interest because it facilitates real-time vision applications due to a large (albeit lossy) reduction in space-complexity [3], and because it represents a prototype for adaptive sampling in a more general setting. In a biological context, primate visual sampling has been demonstrated to be strongly space variant [4], possessing a single high resolution area (fovea) with resolution falling off linearly toward the periphery. Many non-primate species possess an even more exotic visual architecture. Several bird species have multiple foveas [5], and elephants have a magnified representation in the region of their trunk to facilitate "eye-trunk" coordination [6]. Computer vision systems in which the architecture and spatial sampling is adaptively tailored to the specific problem domain may well follow this design path. Thus, it is of importance to develop a universal approach to visual representation which is not implicitly dependent on a regular Cartesian grid. Representations of image data on graph theoretic structures provide one such route to a universal sampling and topology for visual sensing, since it separates the topological (connectivity) from the geometric (sampling arrangement of visual space) aspects of the sensor.

This paper addresses the problem of how to interpolate nodal data on a graph, and then demonstrates applications to image processing. An algorithm is presented that allows interpolation from known values on the nodes of a graph to missing data in such a way that the interpolated values are "smooth". The method is to solve the combinatorial Laplace equation with Dirichlet boundary conditions given by the known values. A solution to the combinatorial Laplace equation has several desirable properties in the context of an interpolation method (see below). Both isotropic and anisotropic interpolation are handled similarly. Furthermore, use of the algorithm is independent of the dimension in which a graph is embedded. Combinatorial differential operators corresponding to the vector calculus operators Div and Grad are used to develop combinatorial versions of the Laplace and Laplace-Beltrami operators. This homology between continuum and combinatorial (graph) algorithms is well known in the literature of circuit theory, mechanical engineering, and related areas in which discretizations of partial differential equations play a central role [7]. The solution to the Laplace equation is analogous to solving an equivalent electrical circuit. The solution to problems of this type, as first noted by Maxwell [8, 9], represents a minimal power dissipation state in the electrical circuit formulation, as shown by Dirichlet's Principle [10, 11]. An application of these ideas to isotropic and anisotropic image interpolation is presented, and a brief discussion of the relation of this work to anisotropic diffusion is outlined.

2 Dirichlet problem

Solving the Laplace equation in order to "fill-in" missing values has been described in the context of digital elevation models [12, 13], image editing [14], and is even used by the ™MATLAB function `roifill.m` to fill in regions of missing data in images. What is new about the present work is the generalization of this interpolation concept to arbitrary geometries, topologies and metrics, i.e., to an image representation based on an arbitrary graph rather than on the familiar uniform raster.

2.1 Definitions

The **Dirichlet integral** may be defined as

$$D[u] = \frac{1}{2}\int_{\Omega} |\nabla u|^2 d\Omega, \tag{1}$$

for a field u and region Ω [15]. This integral arises in many physical situations, including heat transfer, electrostatics and random walks.

A **harmonic function** is a function that satisfies the **Laplace equation**

$$\nabla^2 u = 0. \tag{2}$$

The problem of finding a harmonic function subject to its boundary values is called the **Dirichlet problem**. The harmonic function that satisfies the boundary conditions minimizes the Dirichlet integral, since the Laplace equation is the Euler-Lagrange equation for the Dirichlet integral [11]. In a graph setting, points for which there exist a fixed value (e.g., data nodes) are termed **boundary points**. The set of boundary points provides a Dirichlet boundary condition. Points for which the values are not fixed (e.g., missing data) are termed **interior points**.

2.2 Interpolation

Solutions to the Laplace equation with specified boundary conditions are harmonic functions, by definition. Finding a harmonic function that satisfies the boundary conditions may be viewed as a method for finding values on the interior of the volume that interpolate between the boundary values in the "smoothest" possible fashion [15]. In this section, we discuss the properties of harmonic functions that make them useful for interpolation, defining smoothness in terms of extremal solutions to the Dirichlet integral.

From a physical standpoint, one may think of a heat source with a fixed temperature at the center of a copper plate and a second heat source with fixed temperature on the boundary of the copper plate. The temperature values taken by the plate at every point are those assumed by a harmonic function subject to the internal and external boundaries imposed by the heat sources. In this analogy, the temperatures measured on the inside of the copper plate may be viewed as smoothly interpolated between the temperature on the internal heat source and the external heat source. The internal and external heat sources are considered to be *boundary* points, while points on the copper plate for which temperature values are found are *interior* points.

Three characteristics of harmonic functions are attractive qualities for generating a "smooth" interpolation.

1. The *mean value theorem* states that the value at each point in the interior (i.e., not a boundary point) is the average value of its neighbors [16].

2. The *maximum principle* follows from the mean value theorem. It states that harmonic functions may not take values on interior points that are greater (or less) than the values taken on the boundary [16].

3. The Dirichlet integral is minimized by harmonic functions [10]. This means that the integral of the gradient magnitudes for the system will be minimized, subject to fixed boundary conditions.

2.3 Combinatorial formulation: Differential operators on graphs

A **graph** consists of a pair $G = (V, E)$ with vertices $v \in V$ and edges $e \in E \subseteq V \times V$ with cardinalities $n = |V|$ and $m = |E|$. An edge, e, spanning two vertices, v_i and v_j, is denoted by e_{ij}. A **weighted graph** assigns a (typically nonnegative and real) value to each edge called a **weight**. The weight of an edge, e_{ij}, is denoted by $w(e_{ij})$ or w_{ij}. The **degree** of a vertex is $d_i = \sum w(e_{ij})$ for all edges e_{ij} incident on v_i. Requiring that $w_{ij} > 0$ for all i and j permits interpretation of $1/w_{ij}$ as a distance between nodes v_i and v_j. In other words, nodes connected by an edge with a large weight may be thought of having a short distance between them or as being highly connected. We will see later that in the analogy of an electrical circuit, approaching an infinite weight on an edge spanning two nodes is analogous to approaching an electrical short between the nodes (i.e., weight is interpreted as *conductance*).

One representation [17] of the combinatorial Laplacian operator (see [18, 19, 20, 21] for a discussion of alternatives) is as the $n \times n$ **Laplacian matrix** (see [22] for a review)

$$L_{v_i v_j} = \begin{cases} d_{v_i} & \text{if } i = j, \\ -w_{ij} & \text{if } v_i \text{ and } v_j \text{ are adjacent nodes,} \\ 0 & \text{otherwise.} \end{cases} \tag{3}$$

where $L_{v_i v_j}$ is used to indicate that the matrix L is indexed by vertices v_i and v_j.

Employing the notation of [7], define the $m \times n$ edge-node **incidence**

matrix as

$$A_{e_{ij}v_k} = \begin{cases} +1 & \text{if } i = k, \\ -1 & \text{if } j = k, \\ 0 & \text{otherwise} \end{cases} \tag{4}$$

for every vertex v_k and edge e_{ij}, where each e_{ij} has been arbitrarily assigned an orientation. As with the Laplacian matrix above, $A_{e_{ij}v_k}$ is used to indicate that the incidence matrix is indexed by edge e_{ij} and node v_k. As an operator, A may be interpreted as a combinatorial gradient operator and A^T as a combinatorial divergence [23].

We define the $m \times m$ **constitutive matrix**, C, as the diagonal matrix with the weights of each edge along the diagonal.

As in the continuum setting, the isotropic combinatorial Laplacian is the composition of the combinatorial divergence operator with the combinatorial gradient operator, $L = A^T A$. The constitutive matrix may be interpreted as representing a metric. In this sense, the combinatorial Laplacian generalizes to the combinatorial Laplace-Beltrami operator [24] via $L = A^T CA$. The case of a trivial metric, (i.e., equally weighted, unit valued, edges) reduces to $C = I$ and $L = A^T A$.

Table 1 summarizes the relationship of familiar vector calculus operators to the combinatorial graph theoretic operators defined above and Table 2 summarizes the relationship of equations in both domains.

With these definitions in place, we can determine how to solve for the harmonic function that interpolates values on free ("interior") nodes between values on fixed ("boundary") nodes.

A combinatorial formulation of the Dirichlet integral (1) is

$$D[u] = \frac{1}{2}(Au)^T C(Au) = \frac{1}{2}u^T Lu \tag{5}$$

and a combinatorial harmonic is a function u that minimizes (5). Since L is positive semi-definite, the only critical points of $D[u]$ will be minima.

If we want to fix the values of boundary nodes and compute the interpolated values across interior nodes, we may assume without loss of generality that the nodes in L and u are ordered such that boundary nodes are first and interior nodes are second. Therefore, we may decompose equation (5) into

$$D[u_i] = \frac{1}{2}\left[u_b^T u_i^T\right]\begin{bmatrix} L_b & R \\ R^T & L_i \end{bmatrix}\begin{bmatrix} u_b \\ u_i \end{bmatrix}$$

$$= u_b^T L_b u_b + 2u_i^T R^T u_b + u_i^T L_i u_i. \quad (6)$$

where u_b and u_i correspond to the potentials of the boundary and interior nodes respectively. Differentiating $D[u_i]$ with respect to u_i and finding the critical point, yields

$$L_i u_i = -R^T u_b, \quad (7)$$

which is a system of linear equations with $|u_i|$ unknowns. If the graph is connected, or if every connected component contains a boundary node, then equation (7) will be nonsingular [17]. Although various methods exist for solving a system of linear equations [25, 26], the conjugate gradient method is arguably the best in terms of speed and parallelization [27]. Conjugate gradients requires one sparse matrix multiply per iteration, which is bounded above by $d_{\max}s$, where $d_{\max}$ is the maximum degree of an interior node and s is the cardinality of the set of interior nodes. Assuming a constant number of iterations are required for convergence and that the maximum degree is independent of the number of nodes (e.g., a 4-connected lattice), the time complexity of the algorithm is $\mathcal{O}(s)$.

Combinatorial harmonic functions arise in a wide variety of applications, playing a central role in systems of springs [7], the stress and strain of connected beams [7], Markov chains [28] and electrical circuits [28]. As an example, we will examine the application domain of electrical circuits. The other contexts are essentially identical, differing mainly in language and physical meaning of the respective equations (see [7] for a full discussion). The electrical metaphor, however, is of greater interest in the present context since there is some chance that a VLSI implementation of these methods is possible in terms of the equivalent circuits presented here.

With the notation above, the three main laws governing circuit theory may be written as

$$A^T y = \quad f \qquad \text{(Kirchhoff's Current Law)} \quad (8)$$

$$Cp = \quad y \qquad \text{(Ohm's Law)} \quad (9)$$

$$p = \quad Ax \qquad \text{(Kirchhoff's Voltage Law)}, \quad (10)$$

where f represents current sources at the nodes, p the potential drop (voltage) across a branch, x is the potential at a node and y is the current through a

Operator	Vector calculus	Combinatorial
Gradient	∇	A
Divergence	$\nabla\cdot$	A^T
Curl	$\nabla\times\nabla$	K
Laplacian	$\nabla\cdot\nabla$	A^TA
Beltrami	$\nabla\, C\cdot\nabla$	A^TCA

Table 1: Correspondence between continuum differential operators and combinatorial differential operators on graphs. C represents a constitutive matrix relating flux to flow, e.g., a conductivity tensor, a diffusion tensor, a thermal conductivity, a stress-strain tensor, or, in the context of differential geometry, a metric tensor. A is the incidence matrix of the graph representing the topology of the problem. K is the cycle-edge matrix of the graph [7].

branch. The weights on a branch defining C are given by the conductance of the branch (i.e., the reciprocal of the resistance).

The power, P, associated with a circuit may be written as

$$P = \frac{1}{2}y^TC^{-1}y = \frac{1}{2}x^TLx \tag{11}$$

A comparison of equations (5) and (11) demonstrates that the set of electric potentials at the nodes of a circuit is a discrete harmonic function, i.e., those nodes with a fixed potential due to voltage sources or grounding are the *boundary* nodes, the nodes without a fixed potential are the *interior* nodes. Furthermore, the interior nodes assume potentials that minimize (5) (see [28] for extensive discussion of electrical networks, random walks and the Dirichlet integral). If one were to build a circuit with the same topology as a graph, with appropriate voltage sources to encode the boundary values and resistors to encode the weights, the physical solution (i.e., a minimum energy solution) to the interpolation problem would be exactly equal to the nodal potentials of every interior node. Figure 1 illustrates the circuit corresponding to a graph interpolation problem.

Equation	Continuum	Graph
KVL	$\nabla V = E$	$Ax = e$
KCL	$\nabla \cdot J = \frac{d\rho}{dt}$	$A^T y = f$
Ohm's Law	$\sigma^{-1} E = J$	$Ce = y$
Dirichlet Integral	$\frac{1}{2}\int_\Omega \vert\nabla u\vert^2 d\Omega$	$\frac{1}{2} x^T A^T C A x$

Table 2: Correspondence between continuum differential equations and combinatorial differential equations on graphs. Kirchhoff's current law is a quasi-static ($\frac{\partial B}{\partial t} = 0$) approximation to Maxwell's Equation $\nabla \times E = \frac{\partial B}{\partial t}$. Kirchhoff's voltage law follows from the definition of electric field as the gradient of potential. Ohm's Law is a constitutive (phenomenological) law asserting a presumed linear dependence between voltage and current.

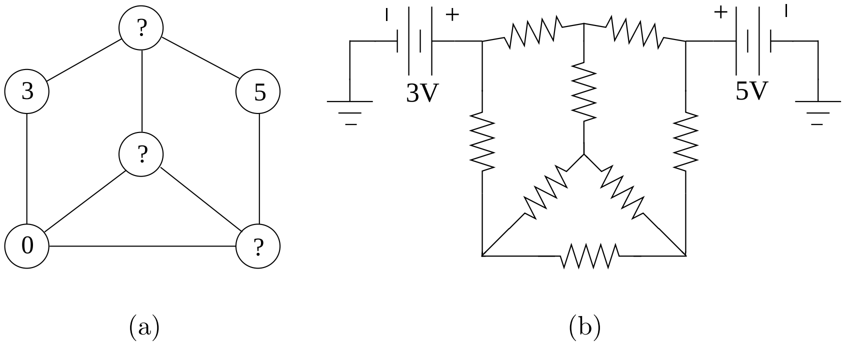

(a)

(b)

Figure 1: Interpolating on a graph with a harmonic is equivalent to setting voltage sources (and grounds) at some nodes and reading off the potentials at nodes which are not fixed. (a) A graph with known values on some nodes and unknown values (indicated with a '?') on other nodes. (b) The equivalent circuit that would produce potentials on the nodes equal to those found by the interpolation method.

3 Results

In this section we demonstrate the interpolation algorithm in the context of image processing.

3.1 Space-variant (foveal) images

In order to demonstrate the use of the interpolation algorithm on an arbitrary graph, we employ an image represented on a graph patterned after the space-variant sampling of the primate foveal visual system [1]. The Lena image was **imported** to the space-variant graph structure by considering the space variant point set as a *resampling* of a Cartesian raster and applying the elliptical Gaussian filters described in [29] (see [30] for more details on this method as applied to space-variant imaging). Other methods for importing a Cartesian image to a space-variant graph could also be used, as long as the output of the importing algorithm was an image field on *nodes*, as opposed to faces or other components of the graph.

Here, we have removed image data in a circular region and performed the interpolation obtained via (7) to fill in the lost values. No weighting was used to compensate for the changing length (if embedded in a Euclidean plane) of the edges. In other words, the interpolation was *isotropic* in the sense that every edge had unit length (corresponding to unit resistors in the circuit analogy). The results may be seen in Figure 2. One can see that the region of the graph for which image values were removed take values that smoothly interpolate between the dark and light regions. However, since no image information is encoded into the structure (i.e., uniform weights), the interpolation algorithm simply fills in the region with a smooth solution. In the next section, it will be shown that encoding image information in the weights and performing an anisotropic interpolation provides a solution that resembles the missing (original) values more than the isotropically interpolated solution.

3.2 Anisotropic interpolation

Anisotropic interpolation may be thought of as weighted interpolation or as finding the potentials in a resistive network in which the resistor values are nonuniform. It is possible to return to the missing data situation of Figure 2 and perform *anisotropic* interpolation using weights derived from the image

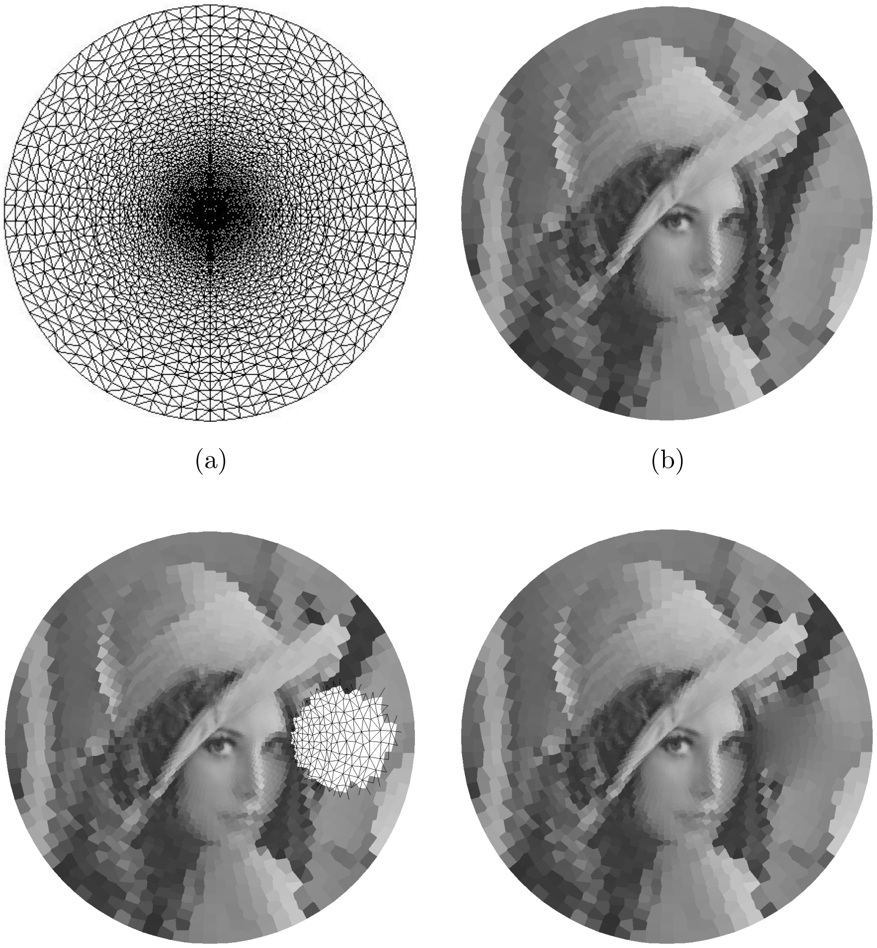

Figure 2: Interpolation of image data on a foveal mesh from which a hole has been cut out. (a) Underlying foveal graph structure. (b) The Lena image imported onto the foveal structure. (c) Foveal image with a hole arbitrarily cut out of it. Underlying graph structure is shown inside the hole. (d) Foveal image with interpolated data in the hole.

values (acquired before the data was removed). We employed a Gaussian weighting function [31]

$$w_{ij} = \exp\left(-\beta |I_i - I_j|\right), \tag{12}$$

where I_i is the image intensity at node (pixel) i and β is a dimensionless parameter that controls the severity of the anisotropy induced by the image intensity. Before using equation (12) the intensity gradients were histogram equalized, since it was determined empirically that if they were not equalized, different values of the parameters would be required to produce similar results for different images.

Weighting the space-variant mesh in accordance with (12) allows for a more accurate reconstruction of the missing data values, as seen in Figure 3.

Building a weighted (i.e., anisotropic) graph for an image using equation (12) allows for a smoothed reconstruction of the original image via anisotropic interpolation from the sampling of a small number of points. These reconstructed images resemble those produced by anisotropic diffusion methods. This is because the solution to the Laplace equation is the steady state of the diffusion equation with specified boundary conditions [28]. The primary difference between diffusion-based methods of image enhancement and those presented here is that diffusion methods approach zero (or constant) when run for infinite time, since Dirichlet boundary conditions are usually not specified in diffusion approaches to image processing. Because of this, diffusion methods (both isotropic and anisotropic) require a stopping condition, while the present method solves directly for a time-independent solution.

This relationship may be seen even more clearly by comparing the equivalent circuit for our interpolation algorithm and the equivalent circuit presented for anisotropic diffusion by Perona and Malik [31]. If one replaced the voltage source at every node in our circuit with an appropriately charged capacitor, then the Perona-Malik equivalent circuit would be obtained exactly. Insofar as similar results are produced for image enhancement tasks with (steady state) anisotropic diffusion and the present method, two advantages of anisotropic interpolation present themselves over diffusion. The first of these is that the solution to the Laplace equation is a steady state solution, while the solution to the diffusion equation depends on time. Therefore, we have no need to iterate and, thus, we circumvent the need to choose a stopping point for the diffusion. Secondly, we can smooth less or smooth more in different areas of the image by decreasing the sampling density in areas

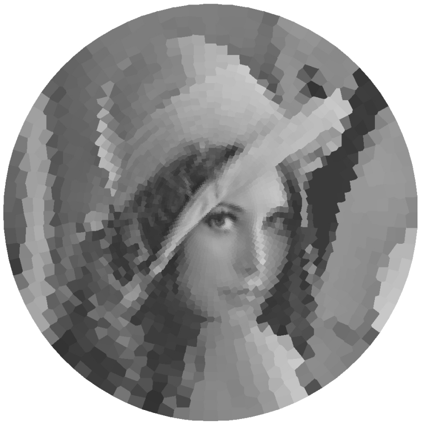

Figure 3: Anisotropic interpolation of image data on a foveal mesh with the same hole as in Figure 2 has been cut out. Weights were determined using $\beta = 30$ (see text for details)

where we desire more smoothing and increasing it in areas where we desire less smoothing.

Figure 4 demonstrates results that are visually comparable to anisotropic diffusion applied to the same image. To generate Figure 4, a 4-connected lattice was generated with weights obtained from equation (12) based on the Lena image. Samples were chosen from relatively uniform areas by computing the square root of the sum of the edge gradients incident on each node. All nodes with a value below a threshold were selected as sample nodes to have their values fixed. The remaining nodes were anisotropically interpolated, given the fixed set. One can see that sharp boundaries are maintained, due to the encoding of image information with weights. Areas of the image with high variability (e.g., the feathers) are smoothed considerably since very few samples were taken, while areas with initially low variability remain uniform.

Of course, it is possible to interpolate by a variety of sampling strategies. Figure 5 illustrates the results of different structured sampling schemes, as well as the flexibility to smooth more or smooth less in different areas of the image. Using the same weights as in Figure 4, but a different choice of samples, it is possible to keep the center of the image true to the original while diffusing out the background or *vice versa*.

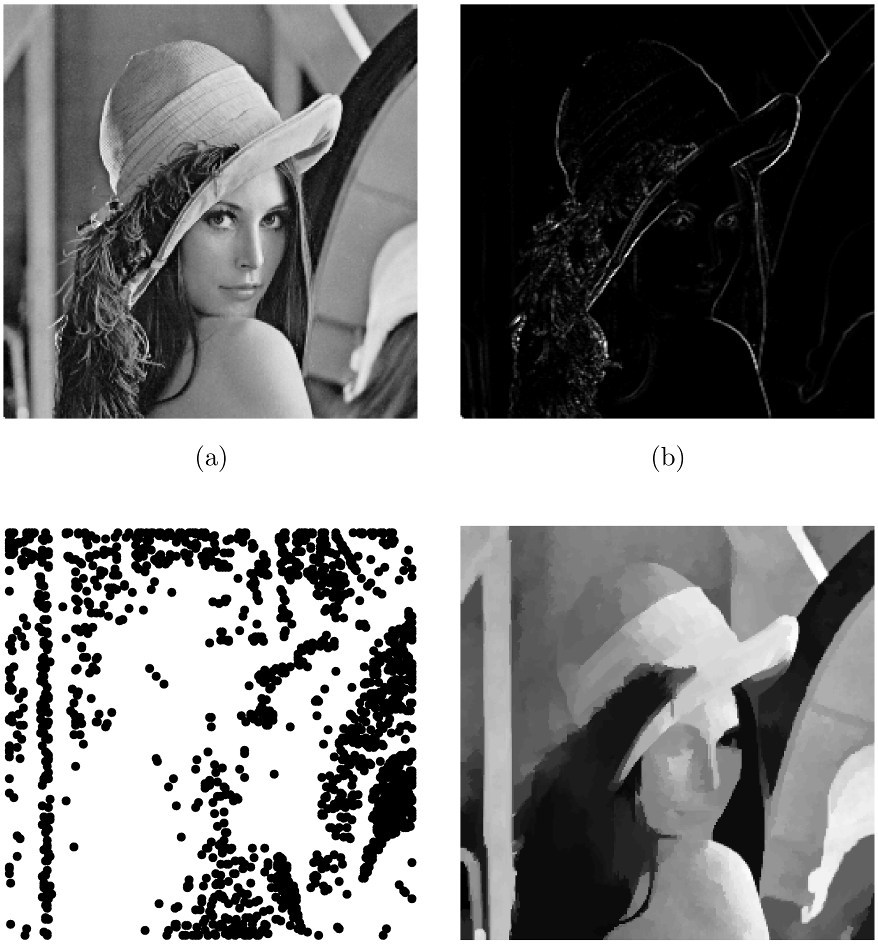

(a)

(b)

(c)

(d)

Figure 4: Anisotropic interpolation of an image based on very sparse sampling. (a) Original Lena image. (b): Magnitude of image gradient. (c): Samples taken from lowest magnitude points. (d): Anisotropically interpolated image.

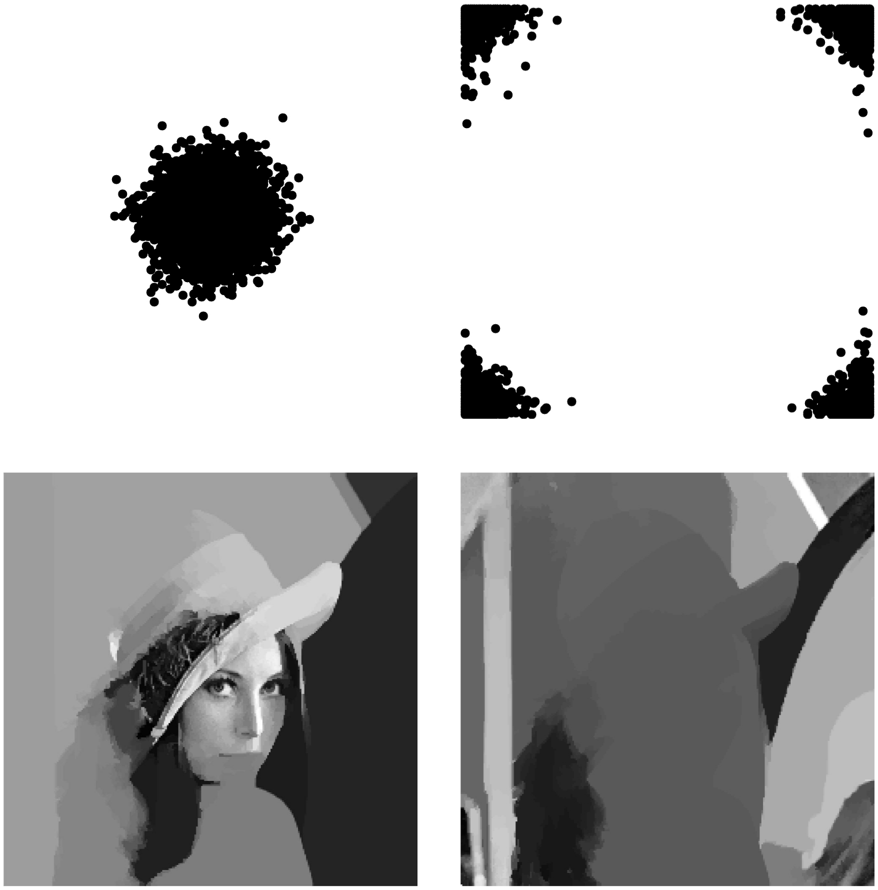

Figure 5: Spatially nonuniform sampling allows for more “diffusion” in some areas over others. This figure demonstrates the effects of two different spatial sampling regimes on the anisotropic interpolation of the Lena image.

4 Conclusion

We have posed the question of how to interpolate nodal values on a graph and proposed a solution based on solving the combinatorial Dirichlet problem. This interpolation method has desirable properties as a result of the mean value theorem and the maximum principle. Furthermore, the method naturally incorporates a metric into the interpolation if anisotropic interpolation is desired. Finally, a circuit analogy was presented which both affords additional intuition into the process as well as holding open the possibility for a VLSI implementation.

Applications of this method to image processing demonstrate its use for filling in missing values in a space-variant image and in the anisotropic smoothing of Cartesian images. Further applications include a smoothing operator for multiresolution reconstruction of graph-based pyramids or three-dimensional interpolation for surfaces. Graphs are general structures that may arise in three dimensions for the purpose of computer graphics [32] or in an arbitrary number of dimensions for data clustering [33]. Since this interpolation method depends only on the topology of the structure and not any information about the dimensionality of the space in which it is embedded, one may interpolate on graph structures existing in arbitrary dimensions possessing an arbitrary metric.

Acknowledgments

The authors would like to thank Jonathan Polimeni for many fruitful discussions and suggestions.

This work was supported in part by the Office of Naval Research (ONR N00014-01-1-0624).

References

[1] Richard Wallace, Ping-Wen Ong, and Eric Schwartz, “Space variant image processing,” *International Journal of Computer Vision*, vol. 13, no. 1, pp. 71–90, Sept. 1994.

[2] Eric L. Schwartz, “Computational studies of the spatial architecture of primate visual cortex:columns, maps, and protomaps,” in *Primary Vi-*

sual Cortex in Primates, Alan Peters and Kathy Rocklund, Eds., vol. 10 of *Cerebral Cortex*. Plenum Press, 1994.

[3] A. S. Rojer and E. L. Schwartz, "Design considerations for a space-variant visual sensor with complex-logarithmic geometry," *10th International Conference on Pattern Recognition, Vol. 2*, pp. 278–285, 1990.

[4] Eric L. Schwartz, "Spatial mapping in the primate sensory projection: analytic structure and relevance to perception," *Biological Cybernetics*, vol. 25, no. 4, pp. 181–194, 1977.

[5] S. P. Collin, "Behavioural ecology and retinal cell topography," in *Adaptive Mechanisms in the Ecology of Vision*, S.N. Archer, M.B.A. Djamgoz, E.R. Loew, J.C. Partridge, and Dordrecht S. Vallerga, Eds., pp. 509–535. Kluwer Academic Publishers, 1999.

[6] Jonathan Stone and Paul Halasz, "Topography of the retina in the elephant *loxodonta africana*," *Brain Behavior and Evolution*, vol. 34, pp. 84–95, 1989.

[7] Gilbert Strang, *Introduction to Applied Mathematics*, Wellesley-Cambridge Press, 1986.

[8] James Clerk Maxwell, *A Treatise on Electricity and Magnestism*, vol. 1, Dover, New York, 3rd edition, 1991.

[9] James Clerk Maxwell, *A Treatise on Electricity and Magnestism*, vol. 2, Dover, New York, 3rd edition, 1991.

[10] Richard Courant, *Dirichlet's Principle*, Interscience, 1950.

[11] Philip M. Morse and Herman Feshbach, *Methods of Theoretical Physics*, McGraw-Hill, 1953.

[12] P. A. Burrough, *Principles of geographical information systems for land resources assessment*, Number 12 in Monographs on soil and resources survey. Clarendon Press, Oxford, 1986.

[13] Joseph Wood and Peter Fisher, "Assessing interpolation accuracy in elevation models," *IEEE Computer Graphics and Applications*, vol. 13, no. 2, pp. 48–56, March 1993.

[14] J. H. Elder and R. M. Goldberg, "Image editing in the contour domain," *IEEE Transactions on Pattern Analysis and Machine Intelligence*, vol. 23, no. 3, pp. 291–296, March 2001.

[15] R. Courant and D. Hilbert, *Methods of Mathematical Physics*, vol. 2 of *Wiley Classics Libary*, John Wiley and Sons, 1989.

[16] L. Ahlfors, *Complex Analysis*, McGraw-Hill, New York, 1966.

[17] Norman Biggs, *Algebraic Graph Theory*, Number 67 in Cambridge Tracts in Mathematics. Cambridge University Press, 1974.

[18] Jozef Dodziuk, "Difference equations, isoperimetric inequality and the transience of certain random walks," *Transactions of the American Mathematical Soceity*, vol. 284, pp. 787–794, 1984.

[19] Jozef Dodziuk and W. S Kendall, "Combinatorial laplacians and the isoperimetric inequality," in *From local times to global geometry, control and physics*, K. D. Ellworthy, Ed., vol. 150 of *Pitman Research Notes in Mathematics Series*, pp. 68–74. Longman Scientific and Technical, 1986.

[20] Bojan Mohar, "Isoperimetric inequalities, growth and the spectrum of graphs," *Linear Algebra and its Applications*, vol. 103, pp. 119–131, 1988.

[21] Fan R. K. Chung, *Spectral Graph Theory*, Number 92 in Regional conference series in mathematics. American Mathematical Society, Providence, R.I., 1997.

[22] Russell Merris, "Laplacian matrices of graphs: A survey," *Linear Algebra and its Applications*, vol. 197,198, pp. 143–176, 1994.

[23] Franklin H. Branin Jr., "The algebraic-topological basis for network analogies and the vector calculus," in *Generalized Networks, Proceedings*, Brooklyn, N.Y., April 1966, pp. 453–491.

[24] Frank W. Warner, *Foundations of Differentiable Manifolds and Lie Groups*, Graduate Texts in Mathematics. Spring-Verlag, 1983.

[25] Gene Golub and Charles Van Loan, *Matrix Computations*, The John Hopkins University Press, 3rd edition, 1996.

[26] Wolfgang Hackbusch, *Iterative Solution of Large Sparse Systems of Equations*, Springer-Verlag, 1994.

[27] J. J. Dongarra, I. S. Duff, D. C. Sorenson, and H. A. van der Vorst, *Solving Linear Systems on Vector and Shared Memory Computers*, Society for Industrial and Applied Mathematics, Philadelphia, 1991.

[28] Peter Doyle and Laurie Snell, *Random walks and electric networks*, Number 22 in Carus mathematical monographs. Mathematical Association of America, Washington, D.C., 1984.

[29] Paul Heckbert, "Fundamentals of texture mapping and image warping," M.S. thesis, University of California at Berkeley, 1989.

[30] Gen-Nan Chen, *Fundamental Algorithms of Space-Variant Vision: Non-Uniform Sampling, Triangulation, and Foveal Scale-Space*, Ph.D. thesis, Boston University, 2001.

[31] Pietro Perona and Jitendra Malik, "Scale-space and edge detection using anisotropic diffusion," *IEEE Transactions on Pattern Analysis and Machine Intelligence*, vol. 12, no. 7, pp. 629–639, July 1990.

[32] G. Taubin, "A signal processing approach to fair surface design," in *Computer Graphics Proceedings. SIGGRAPH 95*, R. Cook, Ed., Los Angeles, CA, Aug. 1995, ACM, pp. 351–358, ACM.

[33] A. K. Jain, M. N. Murty, and P. J. Flynn, "Data clustering: a review," *ACM Computing Surveys*, vol. 31, no. 3, pp. 264–323, Sept. 1999.